Environment International 183 (2024) 108420

Contents lists available at ScienceDirect

Environment International

journal homepage: www.elsevier.com/locate/envint

Full length article

An integrated new approach methodology for inhalation risk assessment of safe and sustainable by design nanomaterials

Giulia Motta [a,b,*], Maurizio Gualtieri [b,*], Rossella Bengalli [b], Melissa Saibene [c], Franco Belosi [d], Alessia Nicosia [d], Joan Cabellos [e], Paride Mantecca [b]

[a] University of Milano Bicocca, Department of Biotechnology and Biosciences, Piazza della Scienza 2, 20126 Milano, Italy
[b] Research Centre POLARIS, Department of Earth and Environmental Sciences, University of Milano Bicocca, 20126 Milano, Italy
[c] Centre for Advanced Microscopy, University of Milano-Bicocca, Piazza della Scienza 2, 20126 Milano, Italy
[d] CNR-ISAC, Institute of Atmospheric Sciences and Climate, National Research Council of Italy, Via Gobetti, 101, 40129 Bologna, Italy
[e] Leitat Technological Center, c/de la Innovació 2, Terrassa, 08225 Barcelona, Spain

ARTICLE INFO

Handling Editor: Adrian Covaci

Keywords:
New approach methodology
Nanoparticle
Risk assessment and hazard
Air liquid interface exposure
Cytotoxicity
Inflammation
Human exposure doses

ABSTRACT

The production and use of nanomaterials (NMs) has increased over the last decades posing relevant questions on their risk after release and exposure of the population or sub-populations. In this context, the safe and sustainable by design (SSbD) approach framework requires to assess the potential hazard connected with intrinsic properties of the material along the whole life cycle of the NM and/or of the nano enabled products. Moreover, in the last years, the use of new advanced methodologies (NAMs) has increasingly gained attention for the use of alternative methods in obtaining relevant information on NMs hazard and risk. Considering the SSbD and the NAMs frameworks, within the ASINA H2020 project, we developed new NAMs devoted at improving the hazard and risk definition of different Ag and TiO2 NPs. The NAMs are developed considering two air liquid interface exposure systems, the Vitrocell Cloud-α and the Cultex Compact module and the relevant steps to obtain reproducible exposures are described. The new NAMs build on the integration of environmental monitoring campaigns at nano-coating production sites, allowing the quantification by the multiple-path particle dosimetry (MPPD) model of the expected lung deposited dose in occupational settings. Starting from this information, laboratory exposures to the aerosolized NPs are performed by using air liquid interface exposure equipment and human alveolar cells (epithelial cells and macrophages), replicating the doses of exposure estimated in workers by MPPD. Preliminary results on cell viability and inflammatory responses are reported. The proposed NAMs may represent possible future reference procedures for assessing the NPs inhalation toxicology, supporting risk assessment at real exposure doses.

1. Introduction

The regulatory system for chemical safety assessment relies largely on *in vivo* approaches while the European Commission is trying to reduce the use of animal models in compliance with the 3R principle (reduction, replacement, and refinement of animal employment for scientific purposes). *In vivo* testing is expensive, time-consuming, and banned in Europe for cosmetic testing (EC No 1223/2009). In this scenario, *in vitro* and *in silico* systems offer progressively reliable and advanced alternatives, also through the development of new approach methodologies (NAMs) for hazard and risk assessment of chemicals. NAMs are strategies based on *in vitro* and *in silico* methods that can provide information on the hazard and risk assessment of chemicals without involving animal testing (ECHA, 2016).

Depending on their structure, NAMs can be a practical tool that allow using available data for designing new experiments and models, with the purpose of generating data that give helpful information for human risk assessment prediction. NAMs may also represent completely new testing strategy that, avoiding the use of animals, deliver reliable data relevant for human physiology and risk assessment (El Yamani et al., 2022). Therefore, through a NAMs approach is possible to improve the understanding of the toxicological mechanisms of a new NM and to evaluate in

* Corresponding authors at: University of Milano Bicocca, Research Centre POLARIS, Department of Earth and Environmental Sciences, Piazza della Scienza 1, 20126 Milano, Italy (G. Motta).
E-mail addresses: g.motta15@campus.unimib.it (G. Motta), maurizio.gualtieri@unimib.it (M. Gualtieri).

https://doi.org/10.1016/j.envint.2024.108420
Received 18 October 2023; Received in revised form 12 December 2023; Accepted 2 January 2024
Available online 3 January 2024

advance its toxicity proposing new materials or refining the NM to lower the undesired negative effects already starting at the early stages of production (Nymark et al., 2020). In the context of new NAMs, data collection through monitoring campaigns, *in silico* modeling, and *in vitro* testing are relevant alternative to classical *in vivo* toxicological approaches.

The use of NAMs for the hazard assessment of chemicals, including nanoparticles (NPs) and nano-enabled products (NEPs), is rapidly increasing, due also to the request of the European Commission to promote new tools for the development of safe and sustainable by design (SSbD) materials (Patinha Caldeira et al., 2022).

Some attempts of introducing NAMs in toxicity testing were done by integrating different strategies. Turley et al. (2019) conducted a comparison between ToxCast and *in vivo* toxicity data to evaluate the program accuracy in predicting the bioactivity of indirect food additives in the context of safety assessment. In another study, Mannerström et al. (2022) employed various *in vitro* tests coupled to a focused analysis of different substances representative of indoor air samples tested. The aim was to establish a connection between the composition of the samples and their biological effects.

The results of these two studies showed that the proposed NAMs need improvements for their direct application to risk assessment; nonetheless, the development of NAMs is important to provide information on the mechanism of action of chemicals, useful for safety screening of new materials and for the definition of novel approaches reducing the use of animals. More recently (Ramanarayanan et al., 2022) proposed a NAMs for pesticides based on an integration between source characterization and *in vitro* models, aiming at defining human exposure concentrations relevant for risk assessment.

In the last decades, the production of new nanomaterials (NMs) increased, since their broad range of properties translates into an extensive variety of practical applications and an attractive commercial impact (Mazari et al., 2021). When nanomaterials are produced or used in various industrial processes, nanoparticles (NPs) can be released into the environment and workers can be exposed. The release of NPs can occur through various routes, such as airborne release, water release or direct contact. The airborne release is the most common during manufacturing processes such as spraying, milling, grinding, or simply by handling of powders. These airborne particles can be dispersed in the environment, inhaled by workers therefore resulting in continuous and prolonged exposure.

In time, some attempts to create a guideline to assess the occupational exposure to airborne NPs have been developed (CEN, 2018; ISO, 2007; OECD, 2015), given that many workers are potentially exposed to these new pollutants by inhalation.

The understanding of the release of NPs during the production process is a valuable resource for conducting risk assessment and implementing effective risk management strategies. The proper evaluation of the environmental concentration of NPs in selected environments, by field monitoring campaign (Boccuni et al., 2020; Trabucco et al., 2022) or laboratory simulations (Natale et al., 2022), can provide the metrics (particles number or mass concentrations) for the evaluation of human exposure by inhalation. The evaluation of human realistic exposure doses is becoming increasingly important in the risk assessment framework, since the effects of NPs on health are affected not only by their physical chemical properties and the route of exposure, but also by the delivered dose (Paur et al., 2011).

Currently performed *in vitro* toxicological studies use unrealistically high concentrations of NPs (Cao et al., 2021; Mittal et al., 2020; Tomankova et al., 2015), while realistic doses might differ and be lower, also considering control measure normally used in workplaces (Ling et al., 2011; Salmatonidis et al., 2019). Therefore, to test realistic doses on an *in vitro* model, it is essential the evaluation, by computational models, of the most likely deposited lung dose(s) of a person exposed to NPs during the production of NMs.

Computational models represent a valid instrument to translate data obtained from field monitoring studies into deposited lung doses. Among the different options, the Multiple Path Particle Dosimetry (MPPD) model (https://www.ara.com/mppd/) is a well-established computational model that allow to calculate the deposition and the clearance of an aerosol of NPs. The model requires input data such as NPs number and mass concentrations, and size distribution to estimate the regional deposition of the NPs and the retention dose of the aerosol. This model is broadly applied with the purpose of assessing the deposition of aerosols in the respiratory tract of humans and laboratory animals (Amoatey et al., 2022; Kuprat et al., 2021; Manojkumar et al., 2019).

The realistic doses calculated by computational models can then be used as reference for providing relevant hazard data thank to the use of *in vitro* models, as closer as possible to the physiology of the target organ, that represent the proper closure to obtain risk assessment data according to NAM and 3R frameworks.

The main aim of this study is to provide a NAM that integrates environmental, modelling, physical chemical, and toxicological information to define the hazard of silver (Ag)- and titanium dioxide (TiO_2)-based NMs designed with different coatings according to a Safe and Sustainable by Design approach (SSbD). The NPs were synthesized with the aims of reducing their toxicity (curcumin coating) and improving their stability (hydroxyethyl cellulose – HEC coating) in suspension still maintaining their antimicrobial (Ag-based NPs) or their photocatalytic properties (Ti-based NPs) with respect to commercial uncoated NPs. Given their commercial interest, these NPs are here tested according to a new NAM procedure. In this study, the lung-retained dose, running the MPPD model, of two selected NPs was determined starting from monitoring campaign data. The model-estimated doses, representative of a chronic human exposure, were used for the exposure of an *in vitro* model of the alveolar space (a contact air liquid interface – ALI co-culture model of A549 and macrophages derived from THP-1 cells) by means of an aerosol exposure system. The alveolar space is expected to be one of the main targets of aerosolized NPs and the region for gas exchanges which physiology is essential for well-being of humans. We also provide information on using two different exposure modules, one based on generation of aerosol droplet allowing deposition by gravitation settling (Vitrocell Cloud α) and the other requiring the ad hoc generation of the desired NPs aerosol but allowing for deposition by random movement and gravitation settling (Cultex Compact Module). The different steps for replicating the proposed NAM are described together with the relevant steps for correctly determining the actual dose of exposure of the *in vitro* model with an ALI exposure system.

2. Materials and methods

2.1. Nanoparticles and reagents

The nanoparticles (NPs) used in this study have a silver (Ag) or titanium dioxide (TiO_2) core with different coatings. Ag NPs are used uncoated (Ag-NKD) or coated with polyvinylpyrrolidone (PVP), hydroxyethyl cellulose (Ag-HECs and Ag-HECp) or curcumin (Ag-CUR). Ag-NKD and Ag-PVP NPs were obtained by Sigma Aldrich (#484059 and #576832, Milano, Italy) while Ag-HEC, already as colloidal suspension (Ag-HECs) or as freeze-dried powder (Ag-HECp), and Ag-CUR were synthesized and provided by the Italian National Research Council (ISSMC-CNR, former ISTEC-CNR, Faenza, Italy). TiO_2 NPs are used without modifications (reference material) or in a nitrogen-doped form (TiO_2-N). Two TiO2 NPs are used, reference TiO_2 NPS (namely, NM-105 supplied by the JRC Nanomaterials Repository) or nitrogen-doped TiO_2 NPs (TiO_2-N provided by Colorobbia, Firenze, Italy and freeze-dried by ISSMC-CNR). All chemicals and reagents were purchased from Sigma Aldrich (Milano, Italy) if not stated elsewhere.

2.2. Preparation of the suspensions

The NPs stock suspensions were prepared in Milli-Q water and used for both characterization and exposure. The NPs provided already as suspensions (Ag-HECs and Ag-CUR) were simply vortexed for 30 s and then diluted in Milli-Q water to reach the final concentration of 1 mg Ag/mL, considering the mass ratio between the Ag core and the surface doping molecules. For the NPs provided in powder form (Ag-NKD, Ag-PVP, TiO_2 and TiO_2-N) the NPs were weighted and diluted in a 50 mL falcon tube with Milli-Q water to reach the concentration of 1 mg of Ag or TiO_2/mL. Then, the tubes were placed in an insulation box filled with ice and sonicated with an ultra-sonicator (Sonopuls HD3100, Bandelin, Berlin, Germany) equipped with a 2 mm probe. NP suspensions were sonicated by applying an electrical power of 40 W for 10 min (with cycles of 1 s pulse and 1 s pause). Ag-HECp NPs were directly diluted in Milli-Q water and vortexed for their high dispersibility in water. Stock suspensions were then further diluted at the final concentration of 100 μg of Ag or TiO_2/mL in Milli-Q water for TEM and DLS characterization or diluted at the desired concentration for deposition efficiency measurement and cell exposures in Milli-Q containing 0.5% of PBS.

2.3. Environmental monitoring campaign and lung deposition doses

A dedicated monitoring campaign was performed at a site of nano enabled products manufacturing as previously reported (Trabucco et al., 2022; Koivisto et al., 2022). Briefly, monitoring of the NPs present in the atmosphere of a pilot plant was performed during normal production phases of nano enabled products (NEPs, in the specific case textiles functionalized with Ag-HECs and TiO_2-N NPs, the other NPs used for toxicological hazard evaluation have been selected for comparative scope, in accordance with the SSbD approach). Particle number size and mass concentrations were obtained in real time by deploying the following instruments an SMPS (L-DMA and CPC mod. 5403, Grimm Aerosol Technik, Ainring, Germany), an OPC (mod 11 D Grimm Aerosol Technik, Ainring, Germany) and an aerosol photometer (DustTrack II mod. 8530, TSI Inc., Shoreview, MN, USA). Monitoring was performed at different distances from the spray coating machinery: at Near Field (NF) position, in proximity to the spray chamber and at heights from 1 to 1.3 m, into the spray coating cabinet and at Far Field (FF) to account for environmental contribution to NPs distribution. NF data, subtracted from interferences from the background, were then used to determine the average size of airborne particles and the average density of the particles. These values were then used to calculate, according to mass concentration values, the expected alveolar retained dose with the MPPD 4.01 software.

2.4. Laboratory lung in vitro model exposure

The *in vitro* co-culture model (paragraph 2.6) was exposed to the different NPs in a Vitrocell® Cloud alpha 12 system equipped with a nebulizer with a droplet MMAD ranging from 4.0 to 6.0 μm and a Quartz Crystal Microbalance (QCM) for the measuring of the deposited mass. For each NP, 200 μL of a suspension, at concentration defined according to the deposition efficiency of the selected NP, were loaded in the nebulizer, and completely aerosolized for 25 s. Then the obtained cloud (NPs plus dispersion medium) was left to settle for 15 min. These procedures were performed under a sterile hood. The exposed cells were then transferred to a CO_2 incubator for 24 h before measuring the biological endpoints.

Between one spray and the next, the nebulizer was cleaned by vaporizing two time consecutively 400 μL of Milli-Q water. Three separate nebulizers were used, one for the negative control (0.5% PBS in Milli-Q), one for the Ag NPs and one for the TiO_2 NPs. The mass contribution of the suspension medium (Milli-Q with 0.5% of PBS) was preliminary measured and then subtracted to the final deposited mass of each NP suspension. Furthermore, to evaluate and reduce the contribution of the PBS salts to the measured mass, without affecting the nebulizer functioning, solutions containing different concentrations of PBS (50, 10, 5 and 0.5%) were nebulized and the deposited mass was measured.

Additional tests were performed with the same co-culture model but with an alternative approach by using the Cultex® RFS Compact module and the Ag-HECs only. The system is not provided with a nebulizing system but allow to expose the cell at a flux of particles, mimicking the inspiration flux. Particles in this model deposit according to their physical properties rather than as total gravimetric deposition such as in the Vitrocell® Cloud alpha 12 system. Briefly, the RFS Compact module was placed under a chemical bench and connected to a sampling line deriving from an expansion chamber (see Figure S6). Particle were generated by a Collison nebulizer (BGI, Inc.) filled with 60 mL of a 100 μg_{Ag}/mL of Ag-HECs particles. Particle size distribution generated by the Collison was preliminary controlled by dedicated experiments (data not shown). Particles nebulized were dried to allow counting with a DiSC mini (Schaefer, Italy) instrument while part of the generated flux was derived to the expansion chamber where temperature was set to 30 °C and relative humidity of the aerosol increased at around 50–60%. The Cultex® module allowed to expose three inserts to the particles arriving from the expansion chamber while three inserts were exposed to the same flux of filtered air. The deposited mass of the generated aerosol is provided according to Gualtieri et al. (2022). The two models differ substantially on the way the particles are dispersed and delivered to the cell culture. The Cloud system relies on vibrating mesh nebulizers having droplet median mass aerodynamic diameter (MMAD, i.e., the average size of particles constituting the deposited aerosol) ranges of 2.5 – 6.0 μm, 2.5 – 4.0 μm and 4.0 – 6.0 μm. The nebulizers therefore generate an aerosol which droplet are at least one order of magnitude bigger than the nebulized NPs. This is functional to depositing most of the mass present in the nebulizer considering gravitational deposition as the main process. On the contrary, the Cultex model is not provided directly with a nebulizing system and different approaches may be selected to provide the aerosol to the system. The aerosol is delivered to the cell culture model by a strictly controlled air flux and the forces that drive particles deposition are both gravitational settling and random movements according to the properties (such as diameter, shape, and density) of the original particle. This main difference in the two system must be carefully considered for a proper understanding of the reported results.

2.5. Deposition efficiency

To define the concentration of the suspension of NPs to be nebulized in the Vitrocell® Cloud alpha 12 system to obtain a desired deposited mass, the measurement of the deposition efficiency is a mandatory step to avoid misinterpretation of the results, above all when comparing different NPs. To measure this parameter the deposited mass of the different NPs is to be evaluated, starting from a suspension at known concentration (150, 250 or 500 μg of Ag or TiO_2/mL in the experiments here reported). To measure the deposited mass the same procedure used for cell exposure was applied except that, after settling of the cloud, the nebulizer chamber was removed for 5 min to let the water to evaporate, a required step for correct mass measurement with a dedicated quartz crystal microbalance (QCM). For the mass measuring, the chamber was placed back and the reading with the QCM started. The microbalance was allowed to stabilize for 5 min and until a stable signal was recorded. The last thirty (30) consecutive values of the stable signal from the QCM were then averaged to obtain the actual deposited mass for the different NPs.

The deposition efficiency of each NP requires the definition of the expected maximal theoretical deposited mass, calculated according to equation (1)

$$expected\ \ dep. = \frac{c^{*}V_{neb}}{A_c} \quad (1)$$

where c is the concentration of a given NP suspension, V_{neb} is the volume of suspension nebulized (200 μL in our experiments) and A_c is the cross-sectional area of the aerosol chamber (141.5 cm^2). A limiting factor to calculate the maximal deposition is the definition of the concentration c for each NPs. This concentration should permit the dispersion of the whole content of NPs without artefacts. According to preliminary experiments, the following suspensions in Milli-Q with 0.5% PBS were used for the different NPs: Ag-NKD suspensions at 500, 250 and 150 μg/mL; Ag-PVP, Ag-CUR, TiO_2 and TiO_2-N suspensions at 250 μg/mL; Ag-HECs and Ag-HECp suspensions at 150 μg/mL.

The actual deposited mass, as measured by the QCM, was then used to determine the deposition efficiency (DE) for each NP according to equation (2).

$$deposition\ \ efficiency\ \ (DE) = \frac{measured\ \ deposited\ \ dose}{expected\ \ deposited\ \ dose}{*}100 \quad (2)$$

Each NP, having specific physical and chemical properties, was tested for its deposition efficiency. DE was then used to determine the concentration of the different suspensions to be nebulized to obtain the desired dose of exposure according to equation (3).

$$Conc = \left[\frac{Dose\ \ of\ \ exposure}{DE}{*}100{*}\frac{Ac}{Vneb}\right] \Big/ 1000 \quad (3)$$

Where *Dose of exposure* is the final desired dose of exposure to be obtained after spraying, *DE* is the efficiency of deposition specific for each NP calculated according to (2), *Ac* is the area of the Vitrocell Cloud chamber, while *Vneb* is the volume of suspension to be nebulized (200 μL in the experiments here reported).

The experiments here reported were performed considering the MPPD derived average retained alveolar doses (Table 1) considering 1, 6 or 12 months of workplace related human exposure.

2.6. Air-Liquid interface Co-culture of A549 and THP-1 derived macrophages

Both cell lines used for the formation of the co-culture were cultivated in OptiMEM medium (Life Technologies Monza, Italy) supplemented with 10% fetal bovine serum (FBS; Gibco Life Technologies, Monza, Italy) and antibiotics (penicillin/streptomycin, 100 U/mL; Euroclone, Pero, Italy). Human alveolar epithelial cells (A549 cell line, ATCC® CCL-185™ ATCC, Manassas, VA, USA) and human monocytes (THP-1 cell line, ATCC® TIB202™) were cultivated in submerged conditions prior co-culture set-up. Cells were maintained in an incubator at 37 °C and 5% CO_2. A549 were seeded on the apical side of the porous membrane (with a pore diameter of 1.0 μm) of 12 well inserts (cellQART, SABEU GmbH & Co. KG, Northeim, Germany) at a density of $5x10^4$ cell/insert and allowed to grow for 48 h. THP-1 cells were differentiated (dTHP-1) for 24 h with 20 ng/mL of Phorbol 12-myristate 13-acetate (PMA). After differentiation, the medium was removed, and cells were allowed to recover for 24 h in fresh medium. The co-culture was then formed by adding differentiated dTHP-1 directly in contact with the A549 cells with a ratio of 1:10. dTHP-1 cells were left to seed for 4 h, then the medium in the apical side of the inserts were removed and fresh medium was added in the basal side of the well. After 24 h of differentiation at the Air-Liquid Interface (ALI), the co-culture was considered established. The exposure of the co-culture to the different NPs was performed as already described.

The morphology of the co-culture was observed through scanning electron microscopy (SEM) using a TESCAN Vega®XM 5136 SEM operating at 20 kV acceleration voltage (Figure S5).

Table 1
Average alveolar retention dose. The doses representative of an exposure of one week shift, 1 month, 6 months and 1 year for the two representative NPs used during the monitoring campaign are reported in the table, the values calculated by the MPPD model are highlighted in grey.

	Average Alveolar Retention dose			
	5 days	**1 month**	**6 months**	**1 year**
Ag-HEC	4.47 ng/cm^2	19 ng/cm^2	116 ng/cm^2	232 ng/cm^2
TiO_2	6.23 ng/cm^2	27 ng/cm^2	162 ng/cm^2	324 ng/cm^2

2.7. Cytotoxicity

The cytotoxicity of the co-culture was assessed through the CyQUANT™ LDH Cytotoxicity Assay (Invitrogen Life Technologies, Monza, Italy). 24 h after the exposure to the NPs, the medium from the basolateral compartments of control and exposed cells was collected and the level of LDH (Lactate Dehydrogenase) was assessed immediately to avoid any loss of activity, following manufacturer's instructions. As a positive control, the Lysis buffer included in the kit was added to an insert for 45 min to lysate all the cells cultured on the insert obtaining the maximal amount of LDH. 50 μL of each sample were transferred in triplicate in a 96 multiwell plate and 50 μL of the reaction mixture were added. The plate was incubated at room temperature and in the dark for 30 min. Then, 50 μL of stop solution were added and the absorbance was measured at 490 nm, with a reference of 680 nm, using a TECAN Infinite M200 Pro microplate reader (TECAN, Männedorf, Switzerland). The cytotoxicity is expressed as relative variation over the positive control performed by complete lysis of the cells.

2.8. Cytokines release

As an index of pro-inflammatory activity, the quantification of three selected cytokines was done through ELISA assays (Invitrogen Life Technologies, Monza, Italy) according to manufacturer's instructions. The quantification of the release of Interleukin 8 (IL-8), Interleukin 6 (IL-6) and Interleukin 1β (IL-1β) was performed on the media of the basolateral side collected from each insert after 24 h of exposure to the NPs. The undernatants were stored at −80 °C until analysis. The absorbance of the samples was measured using a TECAN Infinite M200 Pro microplate reader (TECAN, Männedorf, Switzerland). The concentration of interleukins was calculated based on standard curves and data are shown as fold change compared to the negative control.

2.9. Data collection and statistical analysis

Data of deposition efficiency are expressed as the mean ± standard error of mean (SD) of at least three independent experiments ($N > 3$, if not otherwise stated). Data of the biological analysis are expressed as mean ± standard deviation (SD) of at least three biological independent experiments. For the cytotoxicity, three technical replicas for each biological replicate were analyzed. Statistical analyses were performed using the R software (R Core Team, 2021), applying the one-way ANOVA test followed by Dunnett's post hoc test. The homogeneity of the variance was confirmed by Levene's test. Values of $p < 0.05$ were considered statistically significant.

3. Results

3.1. Environmental monitoring campaign and lung deposition modelling

The particle number size distribution at a factory processing textiles by spray techniques for nano-coating are reported in Trabucco et al. (2022). The data collected were used to determine the measured geometric mean concentration (39 and 94 μg/m^3 for AgHEC and TiO_2-N respectively) and average density (6.5 g/cm^3 and 2.1 g/cm^3 for Ag-HEC and TiO_2-N, respectively) of the particles, while polydisperse particle distributions obtained from field campaign data were used as count

median distribution (CMD). These values were then used in the MPPD 4.01 software to obtain the lung deposited dose also considering clearance (Table 1). A classical shift of 8 h for 5 consecutive days a week was considered for estimating worker exposure. Deposition was modelled in an adult considering a human symmetric lung geometry with 24 consecutive segments, a total lung capacity (TLC) of 5558.09 mL, a functional residual volume (FRC) of 3300 mL, a scaling tree factor of 1.053, a lung distal volume of 2850 mL and a volume of conducting airways of 171.31 mL. The breathing frequency was considered equal to 20 breathing per minute (1.5 sec for inhalation and 1.5 sec for exhalation), the tidal volume was set to 1100 mL and the nasopharyngeal death space equal to 50 mL. The low number and mass concentration of nanoparticles measured at the working area determined a low mass of Ag-HEC and TiO_2 nanoparticles deposited at the alveolar region on daily basis that was in the order of few ng per square cm. These values considering the high density adopted for the calculation may be even lower for other materials with lower density. Considering a cumulative deposition (Table 1), over a year of continuous exposure, the expected retained dose reached the order of hundreds of nanograms (232 and 324 ng/cm^2 for Ag and TiO_2 respectively).

3.2. Deposition efficiency

The measurement of deposition efficiency typical for each NPs is essential to reproduce *in vitro* the deposited dose calculated through the MPPD model.

To calculate the deposition efficiency for each NP, the maximal theoretical deposition was obtained, for different NPs concentrations, according to equation (1) and the results are reported in Table 2.

The actual deposited dose was measured by the QCM for each NP. A preliminary assessment of the mass deposited by the spraying medium (Milli-Q with PBS) was performed to obtain the mass attributable to the selected spraying medium that is to be subtracted to obtain the final NPs mass. The suspending medium, Milli-Q with 0.5% of PBS, was finally selected for NPs exposures and deposition efficiency measurements. The QCM measured deposited doses are reported in Table 3.

The NPs concentration of the suspensions to be sprayed were defined *a priori* based on the peculiar properties of each NP suspension. NPs were characterized for their hydrodynamic properties once in solution, their surface charge (ζ-potential) and their physical properties (size and shape) (see supplementary materials and methods, supplementary results, and supplementary Figure S1 and Table S1). In fact, for some NPs, solutions at high concentration were not compatible with the nebulizing system. As an example, a clogging effect was encountered during nebulization of Ag-HECs and Ag-HECp NPs at the concentrations of 250 and 200 μg/mL (Fig. S3A). The high viscosity of these suspensions determined the deposition over the spraying grid of big aggregates of NPs that impaired a complete and homogeneous nebulization process. Therefore, only suspensions up to 150 μg/mL were nebulized for these NPs. Similarly, after the nebulization of a suspension of 500 μg/mL of Ag-NKD NPs, it was noticed that part of the NPs remained clogged in the mesh of the vibrating membrane (Fig. S3B).

3.2.1. Estimation of deposition efficiency

The results obtained by spraying the different solution were used to calculate the deposition efficiency specific for each NP, according to the equation (2). The different NPs have different deposition efficiency

Table 2
Maximal theoretical deposition for each single nebulization based on the suspension concentration in μg/mL of NPs.

	μg in each spray	μg/cm^2	ng/cm^2
Deposit expected for 500 μg/mL:	100	0.71	707
Deposit expected for 250 μg/mL:	50	0.35	353
Deposit expected for 150 μg/mL:	30	0.21	212

Table 3
Measured deposition of Ag and TiO_2. The results are obtained by spraying different μg/mL of NP to estimate the best conditions. The mass of Ag or TiO_2 was calculated considering the mass ratio of Ag or TiO_2 over the doping molecules in the different NPs (for Ag-HECs the silver is 8.04%, for Ag-HECp it is 7.7% and for Ag-CUR it is 47.5%. For all the other NPs, the amount of Ag or TiO_2 is close to 100%). * = NPs not tested on the biological model.

	μg/mL	PBS (%)	Deposition efficiency (%) ± SD
Ag-NKD	250	0.5	31.03 ± 4.27
Ag-PVP*	250	0.5	50.69 ± 10.73
Ag-HECs	150	0.5	82.81 ± 6.19
Ag-HECp*	150	0.5	64.55 ± 7.60
Ag-CUR	250	0.5	87.11 ± 7.35
TiO_2	250	0.5	73.48 ± 18.15
TiO_2-N	250	0.5	41.27 ± 4.76

Table 4
Deposition efficiency for each suspension nebulized. * = NPs not tested on the biological model.

	μg/mL	PBS (%)	Deposited mass (ng/cm^2) ± SD
Ag-NKD	250	0.5	109.65 ± 15.08
Ag-PVP*	250	0.5	179.11 ± 37.93
Ag-HECs	150	0.5	175.57 ± 13.11
Ag-HECp*	150	0.5	136.85 ± 16.11
Ag-CUR	250	0.5	307.81 ± 25.99
TiO_2	250	0.5	259.66 ± 64.15
TiO_2-N	250	0.5	145.84 ± 16.82

(Table 4) depending on their characteristics. In detail, Ag NPs coated with HEC or CUR have a higher deposition efficiency while Ag-PVP and especially Ag-NKD showed the lower ones. TiO_2 has a deposition efficiency that is much higher with respect to TiO_2-N. These results suggests that the p-chem properties of the NPs could determine the possibility to spray the different solutions. In fact, lower deposition efficiency is found in the NPs with the higher agglomeration tendencies. Although the low number of data available, it was possible to analyse Spearman correlations between the different p-chem and the efficiency of deposition or of deposited mass. The only significant result was a negative association between the deposition of efficiency and the hydrodynamic diameter measure just after the preparation of a working solution. The correlations were negative and significant both considering the hydrodynamic diameter of a solution of 10 μg-ml^{-1} (spearman correlation equal to -0.786, $p < 0.05$) or a solution of 100 μg-ml^{-1} (spearman correlation equal to -0.893, $p < 0.05$).

Based on these results, the concentrations required for each NP to obtain the final exposure doses were calculated (Table 5) and prepared prior to each exposure experiment.

Calculated deposited mass and number of silver NPs in the Cultex module are reported in Table 6. Considering the aerosol size number distribution, the average number and mass of deposited NPs were

Table 5
Concentrations of the suspensions calculated according to (3) for each different NPs to be nebulized to obtain the final exposure dose considering the DE reported in Table 4.

Nanoparticle	Dose of exposure		
	19 ng/cm^2	116 ng/cm^2	232 ng/cm^2
Ag-NKD	43.321 μg/mL	264.486 μg/mL	528.972 μg/mL
Ag-HECs	16.233 μg/mL	99.106 μg/mL	198.213 μg/mL
Ag-CUR	15.432 μg/mL	94.214 μg/mL	188.428 μg/mL
	27 ng/cm^2	**162 ng/cm^2**	**324 ng/cm^2**
TiO_2	25.997 μg/mL	155.981 μg/mL	311.962 μg/mL
TiO_2-N	46.287 μg/mL	277.720 μg/mL	555.440 μg/mL

Table 6
A) Deposited average number and mass calculated for the Cultex RFS Compact module. Average total mass of nebulized particles is in the order of 9.0 + 1.6 ng per square centimetre, while total deposited number where in the order of 1.7*10 + 06 + 3.0*10 + 05 particles per square centimetre. Mass deposition is also reported as Ag relative deposited mass. B) The relative mass contribution of Ag to the total mass was measure on the Teflon filter placed just before the exhaust exit line (see Figure S6). A 12% contribution of Ag to the total mass of the sampled particle was determined by ICP-OES (details on this procedure may be found in Trabucco et al., (2022).

A	Deposited number (±sd) #/cm²	Deposited mass (±sd) µg/cm²
Total deposition	$1.69*10^{+06}$ ($\pm 2.98*10^{+05}$)	$9.02*10^{-03}$ ($\pm 1.59*10^{-03}$)
Deposition reported as Ag mass	nd	$1.05*10^{-03}$ ($\pm 1.85*10^{-04}$)

B	Total mass concentration (±sd) µg/m³	Total Ag concentration (±sd) µg/m³
Generated particle concentrations	1025.41 (±201.48)	119.39 (±42.54)

calculated. As a reference for mass deposition, the average mass concentration of silver generated by the Collison nebulizer is reported (for details refers to supplementary Figure S6).

3.3. Cytotoxicity

The cytotoxicity of NPs at the exposure doses reported was assessed measuring the levels of LDH released by the cells in the media. The results (Fig. 1) show no significant increase or reduction of LDH in the cells treated with the different NPs. Cytotoxicity from test with the alternative exposure module Cultex RFS model were not significantly changed (data not shown) according to the low exposure doses obtained with the exposure procedure (Supplementary Table S3).

3.4. Cytokines release

At the tested doses, the release of the measured inflammatory mediators IL-8, IL-6 and IL-1β (Fig. 2) was not modulated by the NPs except for TiO_2-N. For this NP, there is a significant decrease of IL-1β release in the media for cells treated with all the tested concentrations. There's also a non-significant increase of IL-6 in cells treated with TiO_2-N. Ag NPs induced no modulation. Similar results were obtained with the Cultex RFS exposure module (data not shown). Noteworthy, ALI exposure of the co-culture model to LPS (positive control for inflammation, dose of exposure 10.42 µg/cm² induced a significant release of IL-8, for more detail supplementary materials and methods and supplementary Figure S8). However, the lack of cytokine release in the cell supernatants may be also related to an actual communication between the cell types in co-culture. In fact, the cytokines released from macrophages may be captured by lung cells receptors, and vice versa, therefore removing them from the supernatant and masking the pro-inflammatory effect of the tested NPs.

3.5. The conceptual framework of the proposed NAM

The conceptual framework of the proposed NAM is based on three main blocks, environment data collection and human exposure dose calculation; *in vitro* model definition and preparation; and laboratory efficiency of deposition; *in vitro* model exposure and biological responses evaluation (Fig. 3). Ambient monitoring at the site (production site here) of interest is performed to collect data on the NPs size number distribution and particle density, if not available, these data are used to run a lung deposition model, the MPPD model in our case. The retained alveolar dose, or the deposited alveolar dose, is therefore modelled and used for defining the exposure doses to be performed under lab-controlled conditions. The definition of the *in vitro* model to be tested may be define according to the specific research interest or the laboratory protocols. Here, the lung alveolar model is obtained according to the protocols previously described: after differentiation of monocytes, dTHP-1 cells are seeded on top of the inserts seeded A549 (ratio of number of dTHP-1:A549 equal to 1:10). Then, the culture medium in the apical side of the insert is removed to let the cells at the ALI for at 24 h.

The lung epithelial model is finally exposed to the NPs through the

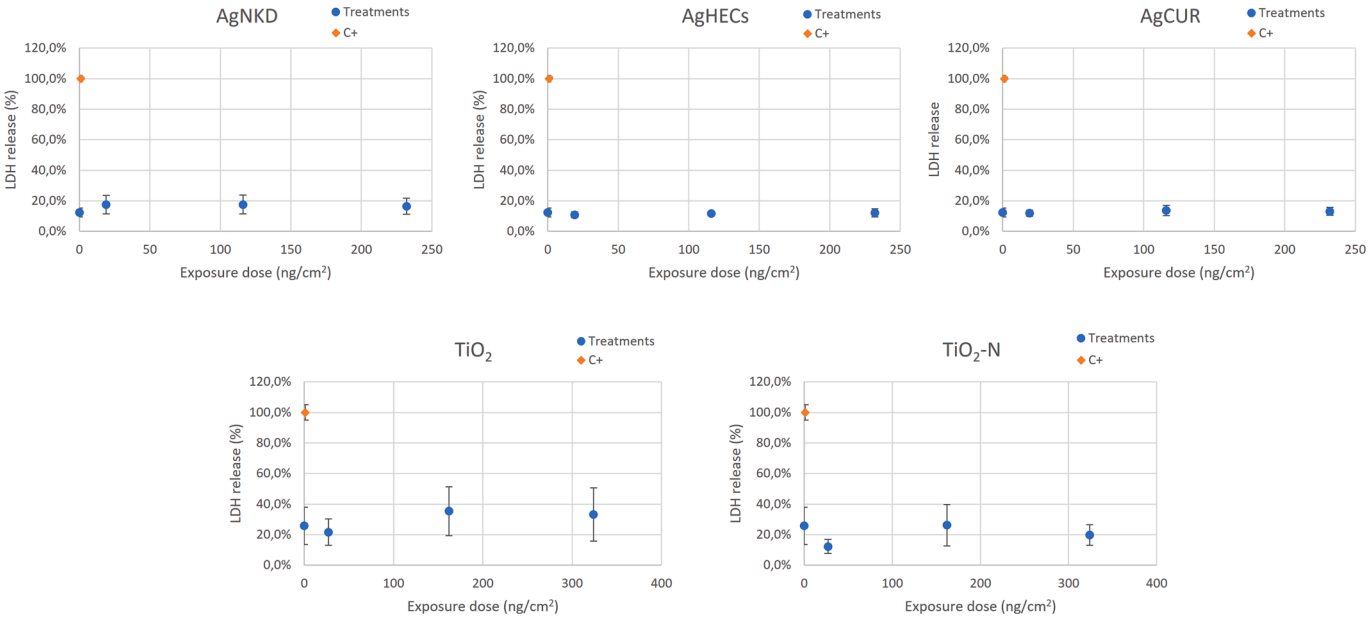

Fig. 1. Cytotoxicity. The graphs show the percentage of LDH release compared to the positive control (black dot equal to 100% cell death). The cytotoxicity was assessed 24 h after NPs nebulization and it was measured through LDH assay. Data are shown as the mean of three independent experiments ± SD. Statistical analysis: one-way ANOVA.

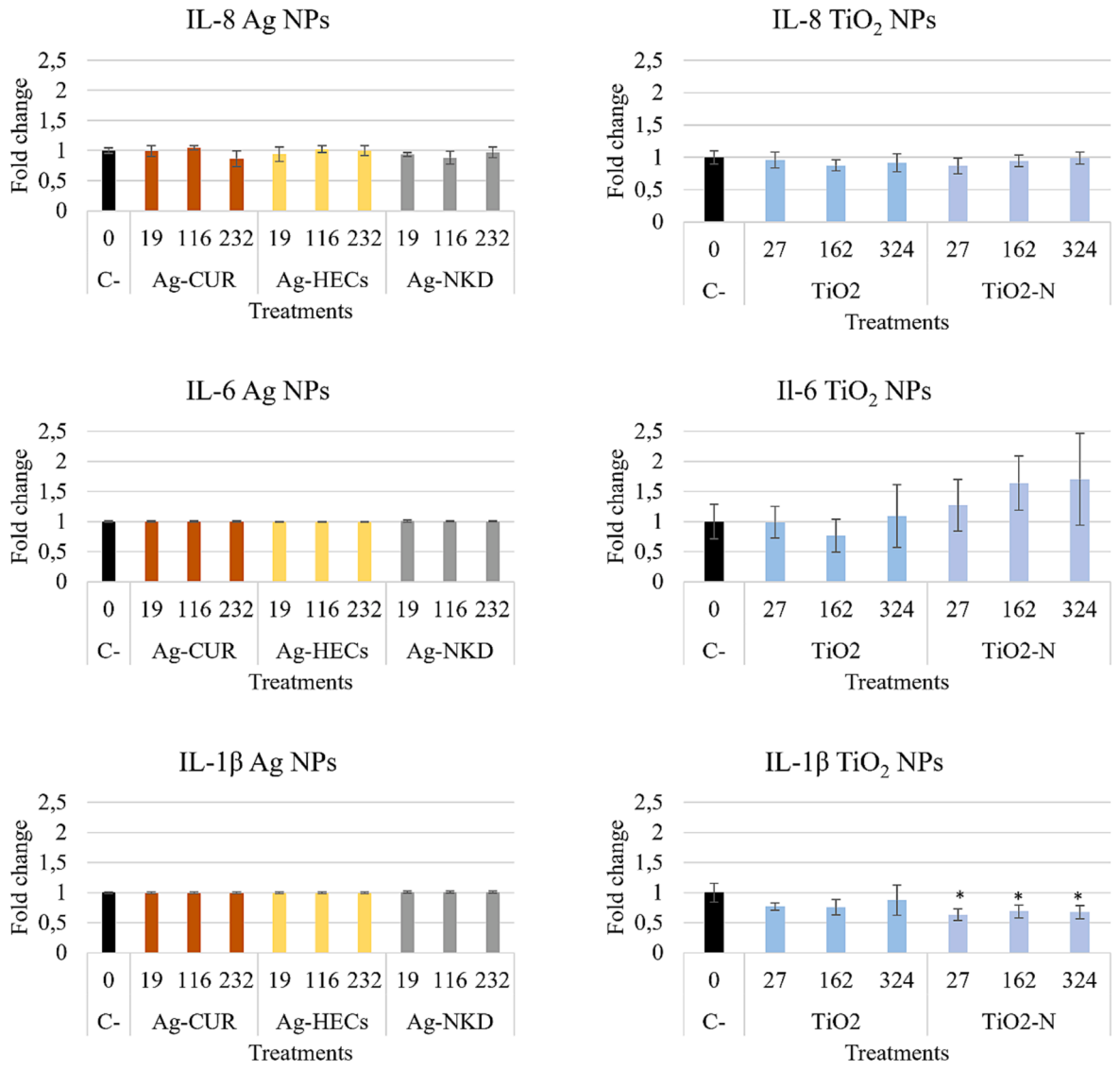

Fig. 2. Cytokines release (IL-8, IL-6 and IL-1β). The release of cytokines in the media was measured 24 h after the NPs nebulization. There is a significant decrease of IL-1β release in cells exposed to TiO_2-N at all tested concentrations. Data are shown as the mean of three independent experiments ± SD. Statistical analysis: one-way ANOVA followed by Dunnett's test. * $p < 0.05$ compared to the control group. As a reference we report here the average and SD of ILs in control cells kept in incubator after ALI differentiation: 492,00 + 67,89 for IL8; 0,99 + 0,13 for IL-6 and 0,95 + 0,21 for IL-1β.

Vitrocell® Cloud alpha 12. After exposure the inserts are place in a CO_2 incubator for the time needed to activate the biological responses (24 h in this case). At the end of the incubation time post-exposure, the lung model is tested for the selected biological outcomes, here: cytotoxicity, cytokine release, and morphology by SEM.

Relevant variation in the proposed NAM may be related to the lung model to be used, to the model used to define the lung deposited or retained dose, to the equipment selected to expose the cells (see for example the procedure reported here for the Cultex Compact module (supplementary materials and methods, supplementary Figure S6 and Figure S7), to the time of incubation to be selected after the exposure and, to the biological endpoints that can take advantage also of omics approaches.

4. Discussion

New nanomaterials (NMs) are continuously developed, and their wide use (Nowack et al., 2011) leads to the release of nanoparticles (NPs) in different environments. The presence of NPs in the environment increases the risk of human exposure by different routes, mostly inhalation, ingestion, and contact. Such exposures can happen also during the use of new NMs or during their production (Kuhlbusch et al., 2018). Furthermore, according to the Safety and sustainable by Design (SSbD) paradigm the safety of a NM has to be assessed during all its life cycle phases.

The proper evaluation of the risk assessment of new NMs is relevant for human health protection therefore, beside environmental, also working place exposure requires specific attention. It has been recently reported (Belosi et al., 2023) that the production processes of nano-enabled material (NEM) may determine local release of NPs in the atmosphere with potential of human exposure. Also, NPs hazard definition should consider, to the best of the knowledge, doses of exposure of biological models that are relevant for humans, to provide data that can be useful in the risk assessment framework (Paur et al., 2011).

Accordingly, we provide here a NAM (Fig. 3) to define the hazard of new Ag and TiO_2 based NMs based on human exposure doses definition (based on monitoring campaign and MPPD modelling) and on an *in vitro* model (representative of the alveolar space) exposed by a well characterized ALI procedure. The proposed NAM represents a step forward since most *in vitro* studies on the toxicological effects of NPs are limited,

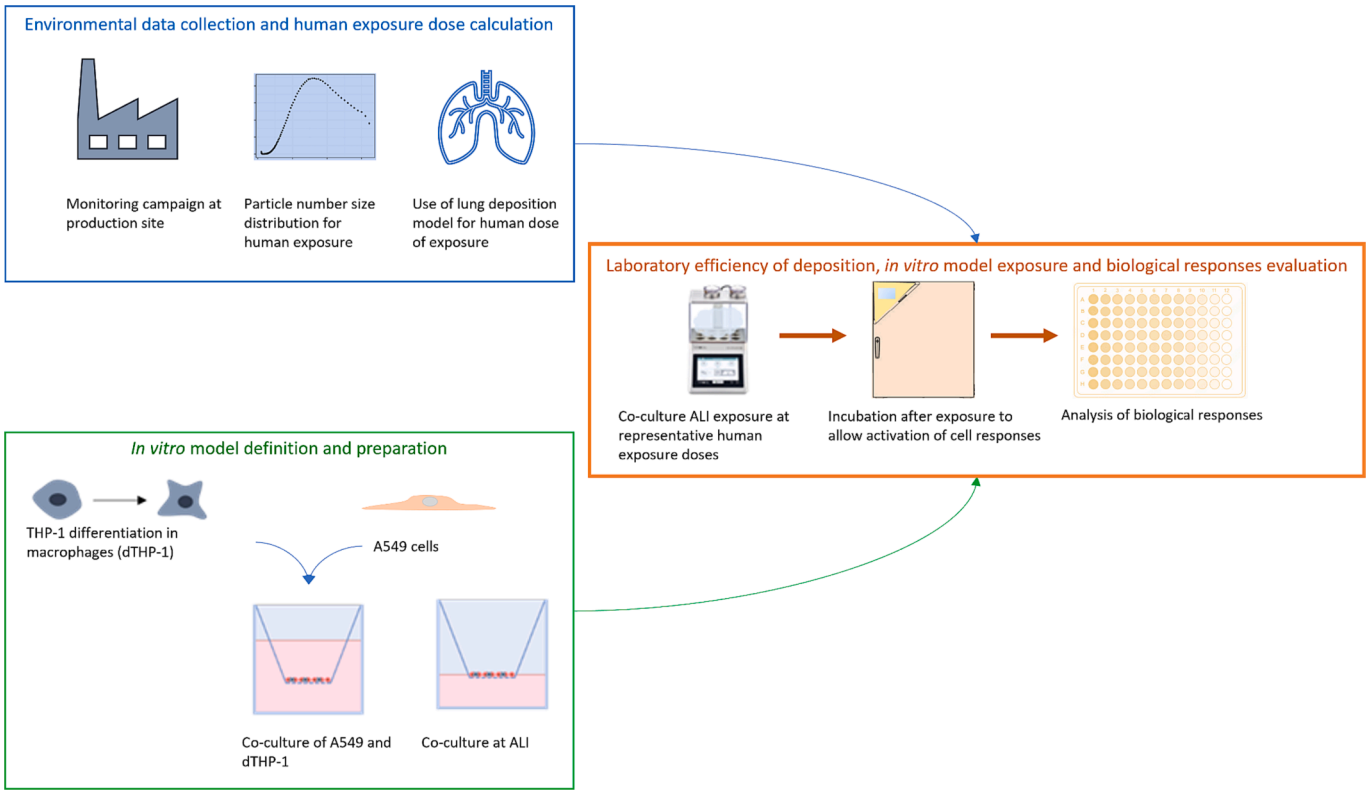

Fig. 3. Workflow of the proposed NAM. The three conceptual blocks required to perform the NAM framework are briefly reported and integrated. The specific solution here adopted are briefly depicted.

since monocultures are exposed in submerged conditions (Andreoli et al., 2021; Lovén et al., 2021) at unrealistic concentrations, without considering lung physiology and complexity (Lenz et al., 2013; Paur et al., 2011). Here, beside using an *in vitro* model representative of the alveolar space, we provide a detailed workflow to adopt ALI exposure systems after preliminary and relevant characterizations (Medina-Reyes et al., 2020; Meldrum et al., 2022). In fact, to get closer to real human exposure conditions, three parameters are important to consider: the biological model, the exposure protocol, and the doses of exposure.

The *in vitro* model should be selected to mimic the interaction between the different cell types of the target organ thus being more reliable model for the pathway of exposure and the biological response. In this context, here we used a co-culture of epithelial cells and macrophages differentiated at the ALI (Cappellini et al., 2020; Loret et al., 2016), although other co-culture models have been proposed (Chary et al., 2019).

The exposure procedure should mimic as much as possible lung deposition: for (nano)particle toxicology, normally adopted models can be summarized in submerged, quasi-ALI, and ALI. For submerged exposure protocols, it is hard, if not impossible, to define the effective dose of NPs that reaches the cells (Upadhyay and Palmberg, 2018), since part of the NPs are absorbed in the walls of the wells or stay in suspension (Cappellini et al., 2020). Also, under submerged exposure protocols the NPs interact with the medium of culture modifying their surface by protein (and other molecules) corona, affecting in the end the interaction between the NPs and the biological model (Ke et al., 2017; Liu et al., 2020; Moore et al., 2015; Zanganeh et al., 2016). Quasi-ALI exposure conditions are seldom used since they take advantage of lung model cultured at the ALI, but the exposure is still obtained by pipetting small volume (tens of microliters, depending on the culture surface) of a solution of NPs dispersed in an appropriate medium. On the contrary, ALI exposure mimics the actual interaction between the lung epithelial cells and the inhaled particles since the NPs interact with the cell membrane at the interface with the air without the need of a medium as vehicle to deliver the NPs to the cells.

Finally, the exposure doses used in the majority of *in vitro* studies are usually in the order of tens of micrograms (Leibrock et al., 2019; Lin et al., 2006). To our knowledge, exposure of an *in vitro* model at ultra-low concentration is reported by Giovanni et al., (2015). The authors used nanograms or picograms of different metal-based NPs to expose, in submerged conditions, murine macrophages showing an increased inflammatory response also at these low concentrations. Nonetheless, this approach, based on submerged cell exposure, can be useful to highlight the overall mechanism of action of the new NPs, it does not allow the prediction of the hazard, since these conditions are far from being representative of real human exposure.

The new integrated methodology here reported overcame these limitations (such as representativeness of the exposure procedure, ALI vs submerged, coherence with expected human exposure doses, relevance of the *in vitro* model for human alveolar space in terms of culturing, ALI vs submerged, and cell types, alveolar cells, and macrophages). Starting from data on NPs released in a work environment during the production of textiles coated with silver (Ag) or titania (TiO_2) NPs (Koivisto et al., 2022), the expected lung retained dose was calculated (MPPD model 4.01 considering working shift of 8 h/day for 5 working days/week) and used as reference parameter to expose the *in vitro* model. The exposure doses here applied are in the order of hundred(s) of ng/cm^2 which, representing an integrated (six months to one year) exposure at the production site, are relevant for human exposure and risk assessment. Tilly et al. (2023) recently reported metal oxide effects at ALI working at concentration of tens to hundreds of micrograms/cm^2; similarly, Medina-Reyes and colleagues (2020) tested TiO_2 based materials in the range of micrograms/cm^2. Interestingly, Wang et al. (2020) reported effects of SiO_2-Ag in a co-culture of A549 and THP-1 cells exposed to 576 ng/cm^2. Future ALI testing should focus on more human relevant exposure doses, to provide hazard data transferable to risk assessment

approaches.

A key step in properly controlling the *in vitro* model exposure doses, and reproducing *in silico* derived human exposure doses, is the evaluation of the deposition efficiency of the different NPs tested. Despite the increasing use of ALI exposure modules, few studies have reported the evaluation of this parameter (Bannuscher et al., 2022; Cristo et al., 2020; He et al., 2021) in spite of the significant difference that different NPs solutions may have and the impact of the effective exposure doses in the biological models.

For example, Lenz et al. (2009) nebulized various solutions (NaCl, $(NH_4)_2SO_4$) and NPs suspensions (ZnO, Au) by means of the air–liquid interface cell exposure system (ALICE) and found a deposition efficiency of 57 ± 0.07% for all the tested substances, showing also a similar efficiency of deposition using different solution concentrations. Similarly, in our exposure model different concentrations of nebulized Ag-NKD showed a stable deposition efficiency (equal to 33.66, 31.16, 35.85% for 500, 250 and 150 μg/mL starting concentrations, respectively). Hu et al. (2020) studied the anti-inflammatory effect of curcumin in both submerged and ALI conditions through the Vitrocell® Cloud Starter Kit aerosol exposure system. Instead of using a QCM, they relied on the autofluorescence of curcumin to determine the delivered dose. In this case, starting from different doses of curcumin (10, 20, 50, 100 μM) they found different deposition factors (0.697, 0.806, 0.545 and 0.668). Bannuscher et al. (2022) used the Vitrocell® Cloud12 system to nebulize concentrations of 0, 125, 250 and 500 μg/mL of DQ_{12} (crystalline silica quartz) and TiO_2 and assessed the deposition efficiency through the QCM. They obtained a linear correspondence between particle concentration and particle deposition, in agreement with our results for Ag-NKD (data not shown) and PBS.

Here we provide an additional interesting observation, i.e., the deposition efficiency may be controlled, rather than by the pristine dimension of the particles, or of the z-potential of the nanomaterial, by the agglomeration tendency that the particles have once dispersed in the working media. Lower is the resulting hydrodynamic diameter, higher will be the final efficiency of deposition. In fact, in our study the deposition of efficiency was higher for Ag-CUR > Ag-HECs > TiO_2 > Ag-HECp > Ag-PVP > TiO_2–N > Ag – NKD, similarly to what observed with the hydrodynamic diameter values that was the lowest for Ag-CUR < Ag-HECs < TiO_2 < Ag-HECp < Ag-NKD < Ag-PVP < TiO_2–N.

The results obtained by assessing cytotoxicity after the nebulization on the co-culture of five of these NPs (Ag-NKD, Ag-HECs, Ag-CUR, TiO_2 and TiO_2-N) at the selected doses indicate the absence of a significant LDH release in the cell medium. The quantification of the release of three selected cytokines also showed no statistical differences between the control and the cells treated with Ag-NKD, Ag-HECs, Ag-CUR and TiO_2. It was observed a reduction of the release of IL-1β in cells treated with TiO_2-N. Similar doses (30 and 278 ng/cm^2) were used by Herzog et al. (2013) to investigate the effects of citrate-coated Ag NPs on a triculture of A549, macrophages and dendritic cells, exposed at the ALI. In agreement with our results, the authors did not observe any significant LDH release from the cells. They also evaluated the production of TNF-α and IL-8 and observed no pro-inflammatory effects at the tested doses. Wang et al. (2020), using a similar co-culture model showed lack of cytotoxicity, by LDH release, using an exposure dose of 576 ng/cm^2, nonetheless the authors reported inflammatory effects. Loret et al. (2016) studied the effects of three different TiO_2-NPs on both a monoculture of A549 and on a co-culture of A549 and macrophages cultured and exposed at the ALI. The doses used in the study were higher (1, 3 and 10 μg/cm^2) to what we report and a higher release of various cytokines (TNF-α, IL-8, IL-6 and IL-1β) on the ALI co-culture was reported. The authors also showed a higher sensibility of the co-culture model with respect to the A549 in the same exposure conditions, and higher effects on the models exposed at the ALI compared to the submerged conditions. Giovanni et al. (2015) tested the pro-inflammatory response of Ag and TiO_2 NPs using concentrations between 10^{-7} μg/mL and 10 μg/mL on a mouse macrophage cell line in submerged conditions. They observed a moderate pro-inflammatory response, starting from the lower concentration in case of TiO_2- treated cells. Even though the lower concentrations used can be compared to the present study, the exposure conditions and the model used are different.

Future steps of improvement are related to possible optimizations of the *in vitro* model since this has been shown to be a relevant factor in properly assessing NPs and other molecules deposition and hazard (He et al., 2021; ; Rothen-Rutishauser et al., 2023). Moreover, for future relevant toxicological studies using this system, prolonged and/or repeated exposures, coupled with the measurement of biological endpoints using omics, are desirable. Also, from a technical point of view exposure allow a proper mimicking of particle deposition in the lungs, therefore considering gravitational settling and random impaction, should be developed, although the required complex nebulization procedure we report here. The possibility to use lung-on-a-chip systems, coupled with other organ-on-a-chip, should be envisaged as well, given the reported predictivity of these models for human health. Finally, the need of generating sound and robust data through NAMs will require further collaboration and integration of expertise from different areas, such as *in vitro* toxicology, human health, air pollution and *in silico* modelling.

5. Conclusions

The NAM here reported allowed for the evaluation of the hazard of new NMs at realistic doses of exposure. Here is shown that different NPs have a different DE depending on their physical chemical properties such as their size and their agglomeration state. Because of that, the determination of the DE is a critical step for properly defining the concentration of NPs to be nebulized, in order to obtain the final doses of exposure. Doses representative of real environmental concentrations, obtained through a field monitoring campaign and *in silico* modelling, allow for the evaluation of NMs safety mimicking the actual human exposure. The choice of the model used to assess NMs toxicity should be done considering the similarity of the model to the target organ to obtain results as reliable as possible. The results of this study suggest the lack of hazard for chronic inhalation exposure and confirm the safety of the NMs and process developed. As additional step, intercomparison among different laboratory should test the framework here presented, as relevant differences among laboratories have been reported when working with ALI exposure modules (Bannuscher et al., 2022; Braakhuis et al., 2023).

Funding

This work was supported by the "ASINA" (Anticipating Safety Issues at the Design Stage of Nano Product Development) European Project (H2020-GA 862444).

CRediT authorship contribution statement

Giulia Motta: Methodology, writing - original draft, Investigation, Visualization. **Maurizio Gualtieri:** Methodology, conceptualization, writing - original draft, Investigation, Visualization, supervision. **Rossella Bengalli:** Investigation, Writing – review & editing. **Melissa Saibene:** Investigation, Writing – review & editing. **Franco Belosi:** Investigation, Writing – review & editing. **Alessia Nicosia:** Investigation, Writing – review & editing. **Joan Cabellos:** Formal analysis, Writing – review & editing. **Paride Mantecca:** Writing – review & editing, supervision, funding acquisition.

Declaration of Competing Interest

The authors declare the following financial interests/personal relationships which may be considered as potential competing interests: All authors reports financial support was provided by European CommissionASINA (Anticipating Safety Issues at the Design Stage of Nano Product Development)European Project (H2020-GA 862444). All

authors reports a relationship with European Commission ASINA (Anticipating Safety Issues at the Design Stage of Nano Product Development)) European Project (H2020-GA 862444) that includes: funding grants. If there are other authors, they declare that they have no known competing financial interests or personal relationships that could have appeared to influence the work reported in this paper.

Data availability

Data will be made available on request.

Acknowledgments

The authors want to thank all the ASINA (Anticipating Safety Issues at the Design Stage of Nano Product Development) European Project (H2020-GA 862444) partners.

Appendix A. Supplementary data

Supplementary data to this article can be found online at https://doi.org/10.1016/j.envint.2024.108420.

References

Amoatey, P., Omidvarborna, H., Al-Jabri, K., Al-Harthy, I., Baawain, M.S., Al-Mamun, A., 2022. Deposition modeling of airborne particulate matter on human respiratory tract during winter seasons in arid-urban environment. Aerosol Sci. Eng. 6, 71–85. https://doi.org/10.1007/S41810-021-00125-2/FIGURES/6.

Andreoli, C., Prota, V., De Angelis, I., Facchini, E., Zijno, A., Meccia, E., Barletta, B., Butteroni, C., Corinti, S., Chatgilialoglu, C., Krokidis, M.G., Masi, A., Condello, M., Meschini, S., Di Felice, G., Barone, F., 2021. A harmonized and standardized in vitro approach produces reliable results on silver nanoparticles toxicity in different cell lines. J. Appl. Toxicol. 41, 1980–1997. https://doi.org/10.1002/JAT.4178.

Bannuscher, A., Schmid, O., Drasler, B., Rohrbasser, A., Braakhuis, H.M., Meldrum, K., Zwart, E.P., Gremmer, E.R., Birk, B., Rissel, M., Landsiedel, R., Moschini, E., Evans, S.J., Kumar, P., Orak, S., Doryab, A., Erdem, J.S., Serchi, T., Vandebriel, R.J., Cassee, F.R., Doak, S.H., Petri-Fink, A., Zienolddiny, S., Clift, M.J.D., Rothen-Rutishauser, B., 2022. An inter-laboratory effort to harmonize the cell-delivered in vitro dose of aerosolized materials. NanoImpact 28, 100439. https://doi.org/10.1016/J.IMPACT.2022.100439.

Belosi, F., Koivisto, A.J., Furxhi, I., de Ipiña, J.L., Nicosia, A., Ravegnani, F., Ortelli, S., Zanoni, I., Costa, A., 2023. Critical aspects in occupational exposure assessment with different aerosol metrics in an industrial spray coating process. NanoImpact 30, 100459. https://doi.org/10.1016/J.IMPACT.2023.100459.

Boccuni, F., Ferrante, R., Tombolini, F., Natale, C., Gordiani, A., Sabella, S., Iavicoli, S., 2020. Occupational exposure to graphene and silica nanoparticles. Part I: workplace measurements and samplings. Nanotoxicology 14, 1280–1300. https://doi.org/10.1080/17435390.2020.1834634/SUPPL_FILE/INAN_A_1834634_SM9739.DOCX.

Cao, Y., Dhahad, H.A., El-Shorbagy, M.A., Alijani, H.Q., Zakeri, M., Heydari, A., Bahonar, E., Slouf, M., Khatami, M., Naderifar, M., Iravani, S., Khatami, S., Dehkordi, F.F., 2021. Green synthesis of bimetallic ZnO–CuO nanoparticles and their cytotoxicity properties. Sci. Reports 2021 111 11, 1–8. 10.1038/s41598-021-02937-1.

Cappellini, F., Di Bucchianico, S., Karri, V., Latvala, S., Malmlöf, M., Kippler, M., Elihn, K., Hedberg, J., Wallinder, I.O., Gerde, P., Karlsson, H.L., 2020. Dry Generation of CeO2 Nanoparticles and Deposition onto a Co-Culture of A549 and THP-1 Cells in Air-Liquid Interface—Dosimetry Considerations and Comparison to Submerged Exposure. Nanomater. 2020, Vol. 10, Page 618 10, 618. 10.3390/NANO10040618.

CEN, 2018. EN 17058 - Workplace exposure - assessment of inhalation exposure to nano-objects and their agglomerates and aggregates [WWW Document]. URL https://www.en-standard.eu/csn-en-17058-workplace-exposure-assessment-of-exposure-by-inhalation-of-nano-objects-and-their-aggregates-and-agglomerates/ (accessed 7.11.23).

Chary, A., Serchi, T., Moschini, E., Hennen, J., Cambier, S., Ezendam, J., Blömeke, B., Gutleb, A.C., 2019. An in vitro coculture system for the detection of sensitization following aerosol exposure. ALTEX - Altern. to Anim. Exp. 36, 403–418. https://doi.org/10.14573/ALTEX.1901241.

Cristo, L. Di, Boccuni, F., Iavicoli, S., Sabella, S., 2020. A Human-Relevant 3D In Vitro Platform for an Effective and Rapid Simulation of Workplace Exposure to Nanoparticles: Silica Nanoparticles as Case Study. Nanomater. 2020, Vol. 10, Page 1761 10, 1761. 10.3390/NANO10091761.

ECHA European Chemicals Agency, Report on the operation of REACH and CLP 2016, 2016.

El Yamani, N., Mariussen, E., Gromelski, M., Wyrzykowska, E., Grabarek, D., Puzyn, T., Tanasescu, S., Dusinska, M., Rundén-Pran, E., 2022. Hazard identification of nanomaterials: In silico unraveling of descriptors for cytotoxicity and genotoxicity. Nano Today 46, 101581. https://doi.org/10.1016/J.NANTOD.2022.101581.

Giovanni, M., Yue, J., Zhang, L., Xie, J., Ong, C.N., Leong, D.T., 2015. Pro-inflammatory responses of RAW264.7 macrophages when treated with ultralow concentrations of silver, titanium dioxide, and zinc oxide nanoparticles. J. Hazard. Mater. 297, 146–152. https://doi.org/10.1016/J.JHAZMAT.2015.04.081.

Gualtieri, M., Berico, M., Grollino, M.G., Cremona, G., La Torretta, T., Malaguti, A., Petralia, E., Stracquadanio, M., Santoro, M., Benassi, B., Piersanti, A., Chiappa, A., Bernabei, M., Zanini, G., 2022. Emission Factors of CO2 and Airborne Pollutants and Toxicological Potency of Biofuels for Airplane Transport: A Preliminary Assessment. Toxics 2022, Vol. 10, Page 617 10, 617. 10.3390/TOXICS10100617.

He, R.W., Braakhuis, H.M., Vandebriel, R.J., Staal, Y.C.M., Gremmer, E.R., Fokkens, P.H.B., Kemp, C., Vermeulen, J., Westerink, R.H.S., Cassee, F.R., 2021. Optimization of an air-liquid interface in vitro cell co-culture model to estimate the hazard of aerosol exposures. J. Aerosol Sci. 153, 105703 https://doi.org/10.1016/J.JAEROSCI.2020.105703.

Herzog, F., Clift, M.J.D., Piccapietra, F., Behra, R., Schmid, O., Petri-Fink, A., Rothen-Rutishauser, B., 2013. Exposure of silver-nanoparticles and silver-ions to lung cells in vitro at the air-liquid interface. Part. Fibre Toxicol. 10, 1–14. https://doi.org/10.1186/1743-8977-10-11/FIGURES/6.

Hu, Y., Sheng, Y., Ji, X., Liu, P., Tang, L., Chen, G., Chen, G., 2020. Comparative anti-inflammatory effect of curcumin at air-liquid interface and submerged conditions using lipopolysaccharide stimulated human lung epithelial A549 cells. Pulm. Pharmacol. Ther. 63, 101939 https://doi.org/10.1016/J.PUPT.2020.101939.

ISO, 2007. ISO/TR 27628: Workplace atmospheres - Ultrafine, nanoparticle and nanostructured aerosols - Inhalation exposure characterization and assessment.

Ke, P.C., Lin, S., Parak, W.J., Davis, T.P., Caruso, F., 2017. A Decade of the Protein Corona. ACS Nano 11, 11773–11776. https://doi.org/10.1021/ACSNANO.7B08008/ASSET/IMAGES/LARGE/NN-2017-08008A_0001.JPEG.

Koivisto, A.J., Del Secco, B., Trabucco, S., Nicosia, A., Ravegnani, F., Altin, M., Cabellos, J., Furxhi, I., Blosi, M., Costa, A., de Ipiña, J.L., Belosi, F., 2022. Quantifying Emission Factors and Setting Conditions of Use According to ECHA Chapter R.14 for a Spray Process Designed for Nanocoatings—A Case Study. Nanomaterials 12, 596. https://doi.org/10.3390/NANO12040596/S1.

Kuhlbusch, T.A.J., Wijnhoven, S.W.P., Haase, A., 2018. Nanomaterial exposures for worker, consumer and the general public. NanoImpact 10, 11–25. https://doi.org/10.1016/j.impact.2017.11.003.

Kuprat, A.P., Jalali, M., Jan, T., Corley, R.A., Asgharian, B., Price, O., Singh, R.K., Colby, S., Darquenne, C., 2021. Efficient bi-directional coupling of 3D computational fluid-particle dynamics and 1D Multiple Path Particle Dosimetry lung models for multiscale modeling of aerosol dosimetry. J. Aerosol Sci. 151, 105647 https://doi.org/10.1016/J.JAEROSCI.2020.105647.

Leibrock, L., Wagener, S., Singh, A.V., Laux, P., Luch, A., 2019. Nanoparticle induced barrier function assessment at liquid–liquid and air–liquid interface in novel human lung epithelia cell lines. Toxicol. Res. (Camb) 8, 1016–1027. https://doi.org/10.1039/C9TX00179D.

Lenz, A.G., Karg, E., Lentner, B., Dittrich, V., Brandenberger, C., Rothen-Rutishauser, B., Schulz, H., Ferron, G.A., Schmid, O., 2009. A dose-controlled system for air-liquid interface cell exposure and application to zinc oxide nanoparticles. Part. Fibre Toxicol. 6, 1–17. https://doi.org/10.1186/1743-8977-6-32/FIGURES/9.

Lenz, A.G., Karg, E., Brendel, E., Hinze-Heyn, H., Maier, K.L., Eickelberg, O., Stoeger, T., Schmid, O., 2013. Inflammatory and oxidative stress responses of an alveolar epithelial cell line to airborne zinc oxide nanoparticles at the air-liquid interface: A comparison with conventional, submerged cell-culture conditions. Biomed Res. Int. 2013 https://doi.org/10.1155/2013/652632.

Lin, W., Huang, Y.W., Zhou, X.D., Ma, Y., 2006. In vitro toxicity of silica nanoparticles in human lung cancer cells. Toxicol. Appl. Pharmacol. 217, 252–259. https://doi.org/10.1016/J.TAAP.2006.10.004.

Ling, M.-P., Chio, C.-P., Chou, W.-C., Chen, W.-Y., Hsieh, N.-H., Lin, Y.-J., Liao, C.-M., 2011. Assessing the potential exposure risk and control for airborne titanium dioxide and carbon black nanoparticles in the workplace. Environmental Science Pollution Research 18, 877–889. https://doi.org/10.1007/s11356-011-0447-y.

Liu, N., Tang, M., Ding, J., 2020. The interaction between nanoparticles-protein corona complex and cells and its toxic effect on cells. Chemosphere 245, 125624. https://doi.org/10.1016/J.CHEMOSPHERE.2019.125624.

Loret, T., Peyret, E., Dubreuil, M., Aguerre-Chariol, O., Bressot, C., le Bihan, O., Amodeo, T., Trouiller, B., Braun, A., Egles, C., Lacroix, G., 2016. Air-liquid interface exposure to aerosols of poorly soluble nanomaterials induces different biological activation levels compared to exposure to suspensions. Part. Fibre Toxicol. 13, 1–21. https://doi.org/10.1186/S12989-016-0171-3/FIGURES/10.

Lovén, K., Dobric, J., Bölükbas, D.A., Kåredal, M., Tas, S., Rissler, J., Wagner, D.E., Isaxon, C., 2021. Toxicological effects of zinc oxide nanoparticle exposure: an in vitro comparison between dry aerosol air-liquid interface and submerged exposure systems. Nanotoxicology 15, 494–510. https://doi.org/10.1080/17435390.2021.1884301/SUPPL_FILE/INAN_A_1884301_SM1109.DOCX.

Manojkumar, N., Srimuruganandam, B., Shiva Nagendra, S.M., 2019. Application of multiple-path particle dosimetry model for quantifying age specified deposition of particulate matter in human airway. Ecotoxicol. Environ. Saf. 168, 241–248. https://doi.org/10.1016/J.ECOENV.2018.10.091.

Mazari, S.A., Ali, E., Abro, R., Khan, F.S.A., Ahmed, I., Ahmed, M., Nizamuddin, S., Siddiqui, T.H., Hossain, N., Mubarak, N.M., Shah, A., 2021. Nanomaterials: Applications, waste-handling, environmental toxicities, and future challenges – A review. J. Environ. Chem. Eng. 9, 105028 https://doi.org/10.1016/J.JECE.2021.105028.

Medina-Reyes, E.I., Delgado-Buenrostro, N.L., Leseman, D.L., Déciga-Alcaraz, A., He, R., Gremmer, E.R., Fokkens, P.H.B., Flores-Flores, J.O., Cassee, F.R., Chirino, Y.I., 2020. Differences in cytotoxicity of lung epithelial cells exposed to titanium dioxide nanofibers and nanoparticles: Comparison of air-liquid interface and submerged cell cultures. Toxicol. Vitr. 65, 104798 https://doi.org/10.1016/J.TIV.2020.104798.

Meldrum, K., Evans, S.J., Vogel, U., Tran, L., Doak, S.H., Clift, M.J.D., 2022. The influence of exposure approaches to in vitro lung epithelial barrier models to assess engineered nanomaterial hazard. 10.1080/17435390.2022.2051627 16, 114–134. 10.1080/17435390.2022.2051627.

Mittal, J., Pal, U., Sharma, L., Verma, A.K., Ghosh, M., Sharma, M.M., 2020. Unveiling the cytotoxicity of phytosynthesised silver nanoparticles using Tinospora cordifolia leaves against human lung adenocarcinoma A549 cell line. IET Nanobiotechnol. 14, 230–238. https://doi.org/10.1049/IET-NBT.2019.0335.

Moore, T.L., Rodriguez-Lorenzo, L., Hirsch, V., Balog, S., Urban, D., Jud, C., Rothen-Rutishauser, B., Lattuada, M., Petri-Fink, A., 2015. Nanoparticle colloidal stability in cell culture media and impact on cellular interactions. Chem. Soc. Rev. 44, 6287–6305. https://doi.org/10.1039/C4CS00487F.

Natale, C., Ferrante, R., Boccuni, F., Tombolini, F., Sarto, M.S., Iavicoli, S., 2022. Occupational Exposure to Silica Nanoparticles: Evaluation of Emission Fingerprints by Laboratory Simulations. Sustain. 2022, Vol. 14, Page 10251 14, 10251. 10.3390/SU141610251.

Nowack, B., Krug, H.F., Height, M., 2011. 120 years of nanosilver history: Implications for policy makers. Environ. Sci. Technol. 45, 1177–1183. https://doi.org/10.1021/ES103316Q/SUPPL_FILE/ES103316Q_SI_001.PDF.

Nymark, P., Bakker, M., Dekkers, S., Franken, R., Fransman, W., García-Bilbao, A., Greco, D., Gulumian, M., Hadrup, N., Halappanavar, S., Hongisto, V., Hougaard, K. S., Jensen, K.A., Kohonen, P., Koivisto, A.J., Dal Maso, M., Oosterwijk, T., Poikkimäki, M., Rodriguez-Llopis, I., Stierum, R., Sørli, J.B., Grafström, R., 2020. Toward rigorous materials production: new approach methodologies have extensive potential to improve current safety assessment practices. Small 16, 1904749. https://doi.org/10.1002/SMLL.201904749.

OECD, 2015. Harmonized tiered approach to measure and assess the potential exposure to airborne emissions of engineered nano-objects and their agglomerates and aggregates at workplaces. Ser. Saf. Manuf. Nanomater. 55, JT03378848.

Patinha Caldeira, C., Farcal, R., Moretti, C., Mancini, L., Rauscher, H., Rasmussen, K., Riego Sintes, J., Sala, S., 2022. Safe and Sustainable by Design chemicals and materials Review of safety and sustainability dimensions, aspects, methods, indicators, and tools, EUR 30991 EN. Publications Office of the European Union, Luxembourg.

Paur, H.R., Cassee, F.R., Teeguarden, J., Fissan, H., Diabate, S., Aufderheide, M., Kreyling, W.G., Hänninen, O., Kasper, G., Riediker, M., Rothen-Rutishauser, B., Schmid, O., 2011. In-vitro cell exposure studies for the assessment of nanoparticle toxicity in the lung—A dialog between aerosol science and biology. J. Aerosol Sci. 42, 668–692. https://doi.org/10.1016/J.JAEROSCI.2011.06.005.

R Core Team 2021 R: A language and environment for statistical computing. R foundation for statistical computing. https://www.R-project.org/, n.d.

Ramanarayanan, T., Szarka, A., Flack, S., Hinderliter, P., Corley, R., Charlton, A., Pyles, S., Wolf, D., 2022. Application of a new approach method (NAM) for inhalation risk assessment. Regulatory Toxicology and Pharmacology 133, 105216. https://doi.org/10.1016/j.yrtph.2022.105216.

Regulation (EC) No 1223/2009 of the European Parliament and of the Council of 30 November 2009 on cosmetic products [WWW Document], n.d. URL https://eur-lex.europa.eu/legal-content/EN/TXT/?uri=CELEX%3A02009R1223-20221217 (accessed 8.7.23).

Rothen-Rutishauser, B., Gibb, M., He, R., Petri-Fink, A., Sayes, C.M., 2023. Human lung cell models to study aerosol delivery – considerations for model design and development. European Journal of Pharmaceutical Sciences 180, 106337. https://doi.org/10.1016/j.ejps.2022.106337.

Salmatonidis, A., Sanfélix, V., Carpio, P., Pawłowski, L., Viana, M., Monfort, E., 2019. Effectiveness of nanoparticle exposure mitigation measures in industrial settings. International Journal of Hygiene and Environmental Health 222 (6), 926–935. https://doi.org/10.1016/j.ijheh.2019.06.009.

Tomankova, K., Horakova, J., Harvanova, M., Malina, L., Soukupova, J., Hradilova, S., Kejlova, K., Malohlava, J., Licman, L., Dvorakova, M., Jirova, D., Kolarova, H., 2015. Cytotoxicity, cell uptake and microscopic analysis of titanium dioxide and silver nanoparticles in vitro. Food Chem. Toxicol. 82, 106–115. https://doi.org/10.1016/J.FCT.2015.03.027.

Trabucco, S., Koivisto, A.J., Ravegnani, F., Ortelli, S., Zanoni, I., Blosi, M., Costa, A.L., Belosi, F., 2022. Measuring TiO2N and AgHEC Airborne Particle Density during a Spray Coating Process. Toxics 10, 498. https://doi.org/10.3390/TOXICS10090498/S1.

Turley, A.E., Isaacs, K.K., Wetmore, B.A., Karmaus, A.L., Embry, M.R., Krishan, M., 2019. Incorporating new approach methodologies in toxicity testing and exposure assessment for tiered risk assessment using the RISK21 approach: Case studies on food contact chemicals. Food Chem. Toxicol. 134, 110819 https://doi.org/10.1016/J.FCT.2019.110819.

Upadhyay, S., Palmberg, L., 2018. Air-liquid interface: relevant in vitro models for investigating air pollutant-induced pulmonary toxicity. Toxicol. Sci. 164, 21–30. https://doi.org/10.1093/TOXSCI/KFY053.

Zanganeh, S., Spitler, R., Erfanzadeh, M., Alkilany, A.M., Mahmoudi, M., 2016. Protein corona: opportunities and challenges. Int. J. Biochem. Cell Biol. 75, 143–147. https://doi.org/10.1016/J.BIOCEL.2016.01.005.